A VARIATIONAL APPROACH FOR RECONSTRUCTING LOW DOSE IMAGES IN CLINICAL HELICAL CT

Synho Do[1]*, W. Clem Karl*[2]*, Mannudeep K. Kalra*[1]*, Thomas J. Brady*[1]*, and Homer Pien*[1]

[1]Massachusetts General Hospital and Harvard Medical School, Dept. of Radiology, Boston, MA
[2]Boston University, Dept. of Electrical and Computer Engineering, Boston, MA

ABSTRACT

Exposure to medical radiation is an important healthcare concern. In this paper we present a variational formulation for image reconstruction from low-dose transmission X-ray CT as well as its application to real clinical data. Our projection domain reconstruction method is based on high-order total variation penalties. We apply the method to clinical neck data obtained from a current 64-channel MDCT helical scanner, where small features and large dynamic range variation are pervasive. The ability to generate high-quality images even at 75% dose reduction is demonstrated. In particular, our approach exhibits image SNR comparable to full-dose filtered backprojection images while avoiding the obvious stair case and blockiness artifacts typically encountered in such methods.

Index Terms— variational approach, iterative reconstruction technique, low dose imaging, cone-beam spiral, MDCT

1. INTRODUCTION

While computed tomography (CT) remains one of the most important diagnostic tools in modern medicine, there is also increasing concern over exposure to medical radiation in general, and the health risks associated with CT radiation exposure specifically [1]. Numerous technical approaches to reducing CT radiation have been developed, including z-axis collimation which prevents the x-ray penumbra from extending beyond the active detector field [2], real-time tube current modulation [3], and improved algorithms. Of particular interest to us is the use of iterative reconstruction techniques (IRTs) to improve image reconstruction quality with respect to the increased noise which occurs in low-dose imaging, including approaches which model the statistical properties of noise in the reconstruction process [4, 5].

Statistical approaches to IRT have been shown to be superior to filtered backprojection (FBP). In general, these approaches have assumed particular statistical distributions of noise, such as the Poisson distribution. In most instances, however, raw CT data have undergone numerous transformations, including negative logarithmic transformation, diffraction and scatter corrections, bow-tie filtering, among others. One result of the mismatch between the data and the assumed model is that the reconstructed images either tends to contain visual artifacts, or small but clinically important features are eliminated. To address these artifacts, additional processing steps are generally required (cf the influence function in [5]). In the case of low-dose CT imaging, where the reduced tube current is manifested in the form of considerably higher noise, the potential appearance of reconstruction artifacts associated with statistical reconstructions is an even greater concern.

Total variation (TV) based functional forms have been extensively examined for their robustness with respect to noise, and especially in the context of edge preservation for image restoration [6, 7, 8]. The basic TV restoration functional is:

$$\hat{u} = \underset{u}{\operatorname{argmin}}\{|\nabla u| + \lambda \|f - u\|^2\}. \quad (1)$$

While under some assumptions this TV functional is equivalent to a MAP estimate corresponding to a MRF model, this variational form does not make explicit statistical assumptions about the data [6].

In the image restoration domain, it has been observed that the non-quadratic penalty term of Eq. 1 generates "blocky" images with staircase-like effects along edges, and that these artifacts can be mitigated through the incorporation of higher order L_1 penalty terms [9].

In this paper, we extend higher-order TV (HOTV) forms to the domain of low-dose CT image formation. We demonstrate that the combination of first- and higher-order TV terms can be used in a variational reconstruction formulation to create high quality images without artifacts. The variational formulation we use includes a comprehensive system model that incorporates models of both a focal spot behavior as well as detector spatial response. We have implemented models specific to a spiral cone-beam clinical 64-channel MDCT system (Siemens Biograph-64). Lastly, we apply this new formulation on clinical data acquired at 1/4 of conventional tube current (i.e., 75% dose reduction) and show the resulting imagery is comparable to conventional FBP-reconstructed images at 100% dose, in clinical neck CT datasets.

2. METHODS

We use a variational functional to solve our tomographic reconstruction problem. Our aim is to improve the quality of low-dose CT images. We obtain a reconstructed image as the solution of the following variational minimization problem:

$$\hat{f} = \arg\min_{f \in BV(\Omega)} E_d(g, f) + \alpha E(f) \tag{2}$$

where $E_d(g, f)$ is a data fidelity term between the desired reconstructed image f and the observed sinogram g, the second term $E(f)$ is the prior or regularization term and α is the weighting term.

For the data fidelity term we assume that the image f and sinogram g are related by the following projection model:

$$g = Hf + n \tag{3}$$

where H is the system projection matrix and n is noise. Due to issues pertaining to the non-linear transformations of the raw signal mentioned previously, we do not make Poisson distributional assumptions regarding the sinograms. In this preliminary work, we use a simple quadratic data fidelity term:

$$E_d(g, f) = \|g - Hf\|_2^2 \tag{4}$$

The system projection matrix H is further decomposed into a geometric projector (P_{geom}), focal spot model (A_{fs}) and active detector response function (A_{det}). Therefore, we model the observation process with an advanced projection system model:

$$H = P_{geom} \cdot A_{fs} \cdot A_{det} \tag{5}$$

For the prior term we use the following energy based on high-order total variation terms:

$$E(f) = \int_\Omega \left[\tau|\nabla f| + (1-\tau)|\nabla^2 f|\right] \, dx\, dy\, dz \tag{6}$$

where $\tau \in [0, 1]$ is a weighting constant, ∇ the gradient operator, ∇^2 the Laplacian, and $\Omega \subset R^3$ is the domain where the image is defined. When $\tau = 1$, this formulation represents the conventional TV (i.e., TV_{D1}). Intermediate values of τ represents a balance of first-derivative preservation of discontinuities and second-order recovery of smooth transition regions (i.e., $TV_{D1,D2}$) [10, 9, 11]. This combination of terms reduces the stair-case artifacts seen in TV-type methods applied to low dose image reconstruction.

3. MATERIALS AND RESULTS

In vivo MDCT raw data was collected and processed by proposed method to examine the image quality that was possible in clinical low-dose situations.

3.1. Data acquisition and scan protocol

A clinical MDCT (Biograph 64 PET/CT scanner, Siemens, Germany) was used to acquire *in vivo* projection data by following an IRB approved research protocol of the Massachusetts General Hospital. The CT neck-imaging protocol was used for all images. Tube voltage was set to 120 KVp and tube current was 420 mA for 100% dose scans (denoted 100D below). Scans were also acquired with a tube current of 105mA, corresponding to 75% reduction of dose (denoted 25D below). Gantry rotation time was 500 $msec$, detector collimation was 0.6 mm, table feed per rotation was 20.2 mm and z-FFS was on. Conventional FBP images were created by the scanner from this data as well as images created with our new HOTV IRT method. In our HOTV reconstruction we used $\tau = 0.5$ to balance the first- and second-order terms based on visual experience. This parameter seemed to work well for the range of examples we used in this preliminary work.

3.2. Image comparison

Fig. 1 shows two standard FBP reconstruction images from the high and low dose data (100D and 25D) as well as the images obtained by our IRT HOTV method on the low dose data (25D) at various iterations. The full dose FBP 100D image shows high Contrast-to-Noise Ratio (CNR) in soft tissue and gives a clean visual impression because of the low noise, where CNR is defined as $(S_A - S_B)/\sigma_0$, with S_A, S_B, and σ_0 the signal intensities of foreground, background, and standard deviation of noise respectively. However, the low dose FBP 25D image is not of diagnostic quality. Specifically, the high level of noise makes it difficult to distinguish transitions between soft tissue structures. In contrast, the improvement produced by our IRT HOTV method can be observed. Our IRT HOTV images exhibit a CNR among different soft tissue regions are comparable to that of the 100D image yet are without staircase and blocky artifacts.

In Fig. 2, we plot the CNR of each of the images in Fig. 1. Note that our IRT HOTV image provides a similar CNR to FBP 100D after 12 iterations while maintaining edge sharpness and without generating additional artifacts. These gains are achieved through the combination of the HOTV formulation as well as the detailed system model described in Sect. 2.

Finally, we do detailed comparison of the FBP 100D, FBP 25D, and our IRT HOTV 25D image after 12 iterations in Fig. 3. We display a whole view of the neck region in Fig. 3(a) and zoomed images in Fig. 3(b), (c), and (d). All the images are displayed in the common contrast window of [-100, 250] HU. Note that there is a small motion between the two different data acquisition due to patient motion, so that the location of small vessels are changed and registration is not perfect.

4. CONCLUSION AND DISCUSSION

We have presented a variational approach for low dose image reconstruction for multi-detector helical CT and shown its application to in vivo data. The method combines a high-order TV-based prior term with an advanced system projection model. The new approach reduces the typical staircase artifacts seen in some IRT-based methods and produces clinical quality imagery. Overall, our IRT HOTV reconstructions from a 25% dose scan yield images of the same quality as conventional FBP images from a 100% dosage scan.

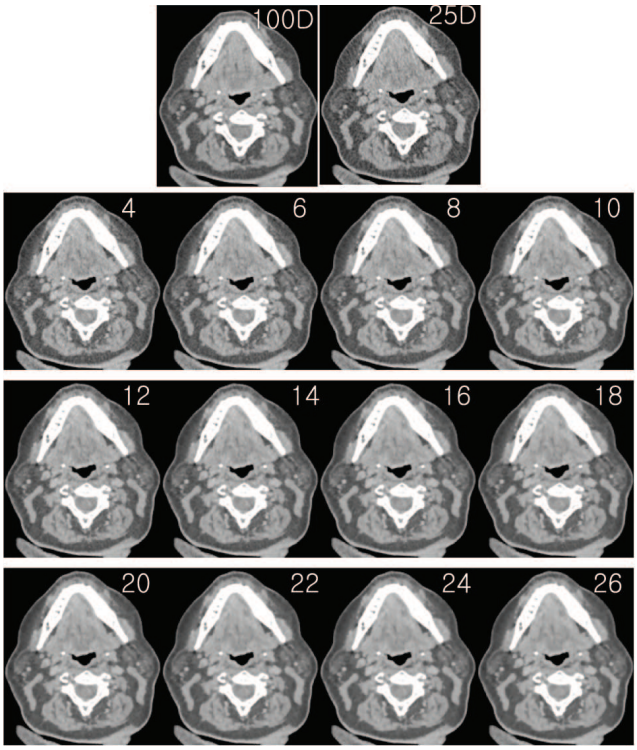

Fig. 1. Image comparison between FBP images and new HOTV IRT images. Top two images show how dosage effects image quality of FBP images(B31f kernel): left 100% Dosage and right 25% Dosage. Twelve HOTV images using 25% Dosage sinogram show how images are changing by the iteration (i.e., 4 through 26). The initial image was a LS(Least-squares) solution, which can be replaced by FBP image.

5. ACKNOWLEDGEMENT

The authors gratefully acknowledge Dr. Rajiv Gupta for ongoing discussions and collaboration, and Christianne Leidecker, Herbert Bruder, and Thomas G. Flohr at Siemens Medical Solutions for providing us with the system concept and design parameters.

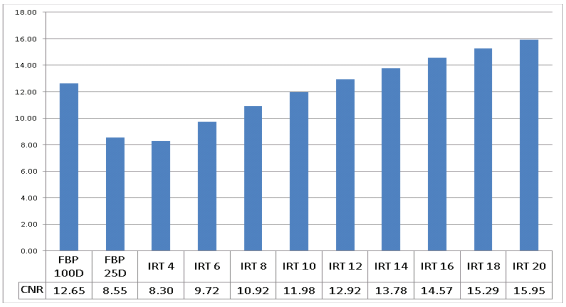

	FBP 100D	FBP 25D	IRT 4	IRT 6	IRT 8	IRT 10	IRT 12	IRT 14	IRT 16	IRT 18	IRT 20
CNR	12.65	8.55	8.30	9.72	10.92	11.98	12.92	13.78	14.57	15.29	15.95

Fig. 2. Contrast to noise ratio (CNR) comparison. CNRs were measured in the images in Fig. 1. After 12 iterations, HOTV image provides a similar CNR to FBP 100%D.

6. REFERENCES

[1] F.A. Mettler, W. Huda, T.T. Yoshizumi, and M. Mahesh, "Effective Doses in Radiology and Diagnostic Nuclear Medicine: A Catalog1," *Radiology*, vol. 248, no. 1, pp. 254, 2008.

[2] T.L. Toth, N.B. Bromberg, T.S. Pan, J. Rabe, S.J. Woloschek, J. Li, and G.E. Seidenschnur, "A dose reduction x-ray beam positioning system for high-speed multislice CT scanners," *Medical Physics*, vol. 27, pp. 2659, 2000.

[3] W.A. Kalender, H. Wolf, and C. Suess, "Dose reduction in CT by anatomically adapted tube current modulation. II. Phantom measurements," *Medical physics*, vol. 26, pp. 2248, 1999.

[4] C.A. Bouman and K. Sauer, "A unified approach to statistical tomography using coordinate descent optimization," *IEEE Transactions on Image Processing*, vol. 5, no. 3, pp. 480–492, 1996.

[5] J.B. Thibault, K.D. Sauer, C.A. Bouman, and J. Hsieh, "A three-dimensional statistical approach to improved image quality for multislice helical CT," *Medical Physics*, vol. 34, pp. 4526, 2007.

[6] L. Rudin, S. Osher, and E. Fatemi, "Nonlinear total variation based noise removal algorithms," *Physica D*, vol. 60, no. 1-4, pp. 259–268, 1992.

[7] T.F. Chan and J. Shen, *Image Processing and Analysis: variational, PDE, wavelet, and stochastic methods*, Society for Industrial Mathematics, 2005.

[8] E.Y. Sidky and X. Pan, "Image reconstruction in circular cone-beam computed tomography by constrained, total-variation minimization," *Phys. Med. Biol*, vol. 53, no. 17, pp. 4777–4807, 2008.

[9] T. Chan, A. Marquina, and P. Mulet, "High-order total variation-based image restoration," *SIAM J. SCI. COMPUT*, vol. 22, no. 2, pp. 503–516, 2001.

[10] A. Chambolle and P.L. Lions, "Image recovery via total variation minimization and related problems," *Numerische Mathematik*, vol. 76, no. 2, pp. 167–188, 1997.

[11] M. Lysaker and X.C. Tai, "Iterative image restoration combining total variation minimization and a second-order functional," *International Journal of Computer Vision*, vol. 66, no. 1, pp. 5–18, 2006.

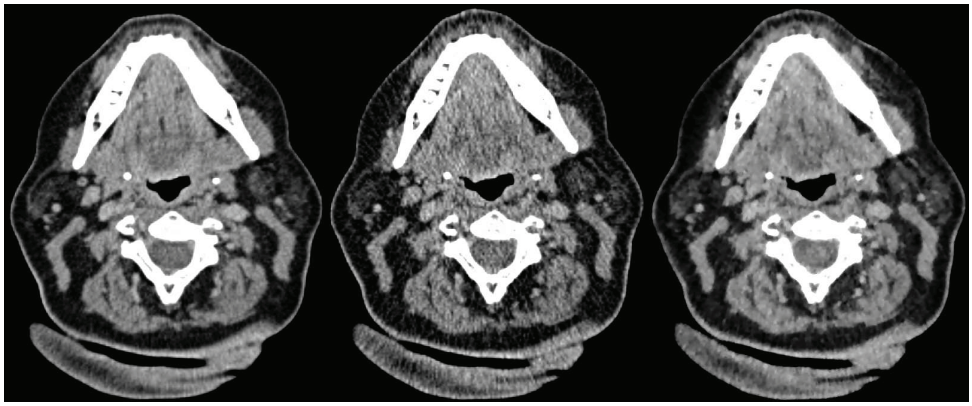

(a) Whole neck view

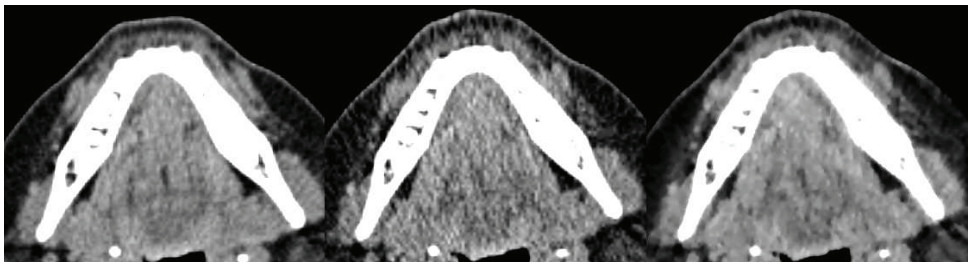

(b)

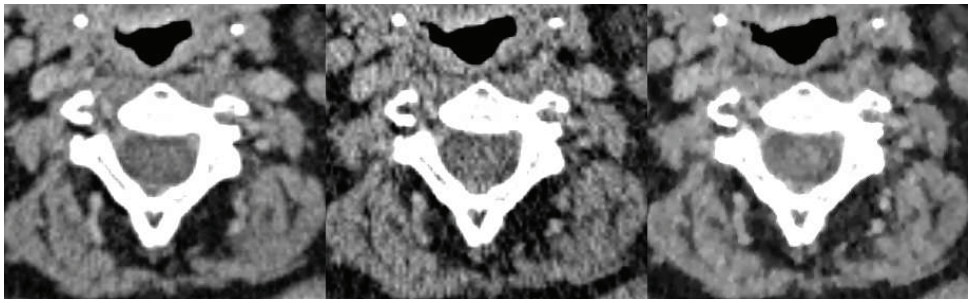

(c)

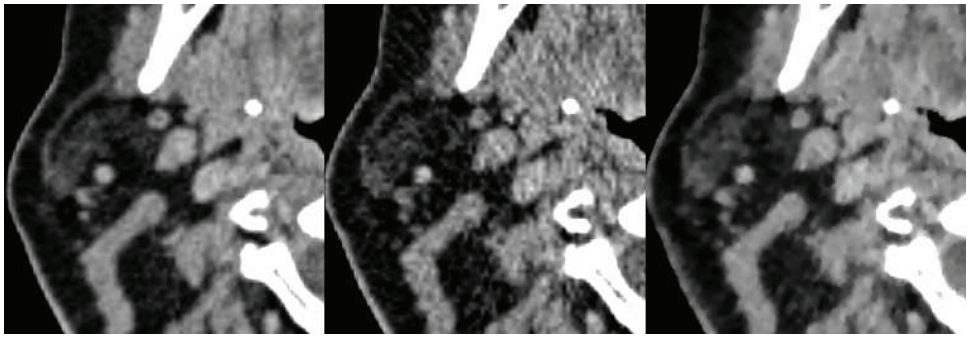

(d)

Fig. 3. A comparison of in vivo images. From left to right, FBP image with normal dosage (100D, $420 \times 0.5 = 210mAs$), FBP image with 75% reduced dosage (25D, $105 \times 0.5 = 52.5mAs$), and our HOTV image from 75% reduced dosage data. All the images are displayed in the same contrast window ([-100, 250] HU) and voxel size ($\Delta x = 0.3mm$, $\Delta y = 0.3mm$, and $\Delta z = 0.6mm$). The images in (b), (c), and (d) show the zoomed images of (a)